Journal of Physiology (2002), **544.2**, *pp.* 417–428
DOI: 10.1113/jphysiol.2002.025171

www.jphysiol.org

Characterization of the A-type potassium current in murine gastric antrum

Gregory C. Amberg, Salah A. Baker, Sang Don Koh, William J. Hatton *, Keith J. Murray *, Burton Horowitz and Kenton M. Sanders

*Department of Physiology and Cell Biology, and *Department of Pharmacology, University of Nevada School of Medicine, Reno, NV 89557, USA*

A-type currents are rapidly inactivating potassium currents that operate at subthreshold potentials. A-type currents have not been reported to occur in the phasic muscles of the stomach. We used conventional voltage-clamp techniques to identify and characterize A-type currents in myocytes isolated from the murine antrum. A-type currents were robust in these cells, with peak current densities averaging 30 pA pF^{-1} at 0 mV. These currents underwent rapid inactivation with a time constant of 83 ms at 0 mV. Recovery from inactivation at −80 mV was rapid, with a time constant of 252 ms. The A-type current was blocked by 4-aminopyridine (4-AP) and was inhibited by flecainide, with an IC_{50} of 35 μM. The voltage for half-activation was −26 mV, while the voltage of half-inactivation was −65 mV. There was significant activation and incomplete inactivation at potentials positive to −60 mV, which is suggestive of sustained current availability in this voltage range. Under current-clamp conditions, exposure to 4-AP or flecainide depolarized the membrane potential by 7–10 mV. In intact antral tissue preparations, flecainide depolarized the membrane potential between slow waves by 5 mV; changes in slow waves were not evident. The effect of flecainide was not abolished by inhibiting enteric neurotransmission or by blocking delayed rectifier and ATP-sensitive K^+ currents. Transcripts encoding Kv4 channels were detected in isolated antral myocytes by RT-PCR. Immunocytochemistry revealed intense Kv4.2- and Kv4.3-like immunoreactivity in antral myocytes. These data suggest that the A-type current in murine antral smooth muscle cells is likely to be due to Kv4 channels. This current contributes to the maintenance of negative resting membrane potentials.

(Received 23 May 2002; accepted after revision 27 July 2002; first published online 16 August 2002)
Corresponding author K. M. Sanders: Department of Physiology and Cell Biology, University of Nevada School of Medicine, Reno, NV 89557, USA. Email: kent@physio.unr.edu

Outward currents through potassium (K^+) channels are the primary means by which excitable cells oppose membrane excitability. In smooth muscles, diverse patterns of electrical activity are determined to a large extent by the complement of K^+ currents present (see Sanders, 1992; Nelson & Quayle, 1995). Many voltage-dependent K^+ conductances have been identified in gastrointestinal (GI) smooth muscles (see Farrugia, 1999; Horowitz *et al.* 1999). An important feature of these currents is the apparent tailoring of voltage dependency such that the currents are available within the range of physiologically relevant voltages.

Transient outward, or 'A-type' currents are voltage-dependent K^+ currents that possess rapid activating and inactivating kinetics and usually become available at negative (subthreshold) potentials. First identified in neurons (Hagiwara *et al.* 1961), A-type currents are generally believed to participate in the regulation of firing frequency (Connor & Stevens, 1971; Tierney & Harris-Warrick, 1992). A-type currents have been identified in a number of non-neural tissues including vascular (Beech & Bolton, 1989) and visceral smooth muscle (see below). A-type currents tend to be a feature of phasic smooth muscles (e.g. portal vein; Beech & Bolton, 1989) and are not usually present in tonic smooth muscles (e.g. coronary artery; Leblanc *et al.* 1994); however, exceptions have been reported (Clapp & Gurney, 1991; Thornbury *et al.* 1992).

A-type currents have been identified in several GI smooth muscles, including guinea-pig colon (Vogalis *et al.* 1993), opossum oesophagus (Akbarali *et al.* 1995), and mouse colon (Koh *et al.* 1999*b*). In isolated guinea-pig colonic (Vogalis *et al.* 1993) and opossum oesophageal myocytes (Akbarali *et al.* 1995), inhibition of the A-type current with 4-aminopyridine (4-AP) shifted the resting membrane potential to more positive potentials and increased the velocity of the action potential upstroke. In murine colon, application of 4-AP to intact preparations abolished the quiescent periods between slow waves and induced a slight depolarization (Koh *et al.* 1999*b*).

Studies of A-type currents have not included phasic muscles of the stomach. In myocytes from guinea-pig antrum, an inactivating outward current (designated I_{to}) was observed (Noack *et al.* 1992); however, as noted by the

authors, this current possessed properties, including relatively slow kinetics, depolarized voltage dependencies, and insensitivity to 4-AP, which precluded classification as an A-type current. In the present study we have performed experiments to test whether A-type currents contribute to the electrical activity of the murine stomach. We have investigated whether the rapidly inactivating K^+ current of antral myocytes has properties consistent with an A-type current (e.g. subthreshold activation, rapid kinetics and sensitivity to 4-AP). We also performed current-clamp studies on myocytes and conventional microelectrode recordings from intact tissues to determine the physiological function of this current in the antrum. In addition, we used pharmacological and molecular techniques to investigate the molecular nature of the A-type current in the antrum.

METHODS

Preparation and collection of isolated myocytes

Smooth muscle cells were prepared from the tunica muscularis of gastric antra of BALB/c mice. Mice were anaesthetized with isoflurane and killed by cervical dislocation. The Institutional Animal Care and Use Committee approved the housing and protocols for the killing of animals. Stomachs were removed and opened along the lesser curvature. The resulting sheets were pinned out in a Sylgard-lined dish, and washed with calcium-free, phosphate-buffered saline (PBS) containing (mM): 125 NaCl, 5.36 KCl, 15.5 NaOH, 0.336 Na_2HPO_4, 0.44 KH_2PO_4, 10 glucose, 2.9 sucrose, and 11 Hepes, adjusted to pH 7.4 with NaOH. The antrum was separated from fundal and corporal regions and the mucosa and submucosa were removed with fine-tipped forceps.

Smooth muscle cell dispersions were prepared as described previously (Amberg *et al.* 2001). Briefly, antra were incubated for 8–12 min at 37 °C in a calcium-free solution supplemented with fatty acid-free bovine serum albumin (4 mg ml^{-1}), papain (20 U ml^{-1}), collagenase (270 U ml^{-1}; Worthington Biochemical, Lakewood, NJ, USA), and dithiothreitol (DTT, 1 mM); the tissue was then washed with calcium-free solution, triturated to form a cell dispersion, and stored at 4 °C.

Dispersed myocytes were collected as described previously (Epperson *et al.* 1999) for RNA isolation (see below). Individual myocytes were selected by the same criteria used during electrophysiological experiments (elongated, spindle-shaped cells, 100–500 μm long, 5–10 μm in diameter) and aspirated into large-bore pipettes. After collecting 60 myocytes, the contents of the pipette were expelled into RNase-free tubes, frozen in liquid nitrogen, and stored at −70 °C.

Voltage-, current-clamp and intracellular microelectrode methods

All experiments were performed at room temperature (22–25 °C) within 6 h of dispersing the cells, using a perfused recording chamber mounted on an inverted microscope. Recordings were performed with an Axopatch 200B system and digitized with a DigiData 1200 A/D converter (Axon Instruments, Union City, CA, USA). Data were digitized at 4 kHz and filtered at 1 kHz using pCLAMP 6 software (Axon Instruments). Fire-polished glass pipettes with resistances of 1–4 MΩ were used. For determination of whole-cell current densities (pA pF^{-1}), cell membrane capacitance was calculated from the time constant of a capacitance current elicited by a 5 mV depolarization from −60 mV. Series resistance (2–5 MΩ) was compensated to at least 70 %. The myocytes were bathed in a nominally calcium-free solution containing (mM): 5 KCl, 135 NaCl, 2 $MnCl_2$, 10 glucose, 1.2 $MgCl_2$ and 10 Hepes, adjusted to pH 7.4 with Tris. The pipette solution contained (mM): 130 KCl, 5 $MgCl_2$, 2.7 K_2ATP, 0.1 Na_2GTP, 2.5 creatine phosphate disodium, 5 Hepes and 10 BAPTA, adjusted to pH 7.2 with Tris.

A junction potential of −4 mV between our bath and pipette solutions was calculated (Barry, 1994). The voltages listed in our protocols and figures are not corrected for this. Only the values of reversal, half-activation and half-inactivation potentials have been corrected.

For intracellular microelectrode experiments, the antral region of the murine stomach (mucosa and submucosa removed) was pinned to the bottom of a Sylgard-lined recording chamber with the mucosal aspect of the circular muscle layer facing upwards. The tissue was maintained at 37 ± 0.5 °C with oxygenated bathing solution consisting of (mM): 118.5 NaCl, 4.5 KCl, 1.2 $MgCl_2$, 23.8 $NaHCO_3$, 1.2 KH_2PO_4, 11.0 glucose and 2.4 $CaCl_2$. The pH of this solution was 7.3–7.4 when bubbled with 97 % O_2–3 % CO_2 at 37 ± 0.5 °C. Circular muscle cells were impaled with glass microelectrodes filled with 3 M KCl with resistances of 70–100 MΩ. Transmembrane potentials were measured with a high-impedance electrometer (WPI duo 773, World Precision Instruments, Sarasota, FL, USA) and outputs were displayed on a Tektronix 2224 oscilloscope (Wilsonville, OR, USA). Electrical signals were recorded digitally using Acqknowledge software (version 3.5.4; Biopac Systems, Santa Barbara, CA, USA).

Data are reported as the mean ± S.E.M., and *n* refers to the number of cells or animals from which recordings were made. Statistical significance was evaluated by Student's *t* test or analysis of variance, as appropriate. *P* values less than 0.05 were considered significant. Methods of curve fitting were performed using pCLAMP 6 (Axon Instruments) or GraphPad Prism (GraphPad Software, San Diego, CA, USA).

Total RNA isolation and PCR

Total RNA was isolated from isolated antral myocytes using the SNAP Total RNA isolation kit (Invitrogen, Carlsbad, CA, USA), according to the manufacturer's protocol. First-strand cDNA was prepared from the total RNA using the Superscript Reverse Transcriptase kit (Gibco, Gaithersburg, MD, USA). A sample (1 μg) of total RNA was reverse transcribed with 200 units reverse transcriptase in a 20 μl reaction mixture containing 25 ng oligo-dT primer, 500 μM each dNTP, 75 mM KCl, 3 mM $MgCl_2$, 10 mM DTT and 50 mM Tris-HCl (pH 8.3). For the control, PCR primers specific for β-actin (GenBank accession no. V01217) nucleotides 2383–2402 and 3071–3091 were used to establish that the cDNA prepared above was non-genomic. The β-actin-specific primers amplified only the intron-less amplification product from all cDNA samples, indicating that these preparations were free of genomic DNA contamination (data not shown).

The cDNA reverse transcription products were amplified with primers specific for Kv4.1 (accession no. M64226) nucleotides 1538–1559 and 1632–1653, Kv4.2 (accession no. AF107780) nucleotides 1529–1549 and 1619–1639, Kv4.3 (accession no. AF107781) nucleotides 1398–1418 and 1553–1573, potassium-channel-interacting protein (KChIP) 1 (accession no. AB075041) nucleotides 126–145 and 270–289, KChIP2 (accession no. AB044570) nucleotides 494–513 and 664–683, KChIP3 (accession no. AF287733) nucleotides 176–195 and 324–343, KChIP4 (accession no. AF305071) nucleotides 229–250 and 394–414, and β-actin

(accession no. V01217) nucleotides 2206–2223 and 2385–2402 by PCR using AmpliTaq Gold reagents (PE Applied Biosystems, Foster City, CA, USA). The amplification protocol was as follows: 95 °C for 10 min to activate the AmpliTaq polymerase, followed by 40 cycles of 95 °C for 15 s and 60 °C for 1 min. Aliquots of the PCR reactions were analysed by 2 % agarose gel electrophoresis and visualized by ethidium bromide fluorescence. PCR amplification products from each primer pair were extracted and identities confirmed by DNA sequencing. Real-time PCR was used to quantify the relative expression levels of Kv4 and KChIP isoforms using SYBR Green I as the fluorescent probe on an ABI 5700 sequence detector (PE Applied Biosystems). Real-time PCR was performed in triplicate using the same amplification protocol described above. Reaction mixtures lacking cDNA (no-template controls) were included during each session to assess contamination and non-specific amplification. To examine Kv4 and KChIP primer efficiencies, standard curves were generated for each primer pair by regression analysis of PCR amplifications on $\log_{10}$ serial dilutions of cDNA. For each Kv4 and KChIP isoform, the β-actin standard curve was used to determine the relative abundance of each transcript, which was then normalized to the amount of β-actin transcript present within the same sample (Walker *et al.* 2001).

Immunohistochemistry

Mouse antrum was collected and flushed with phosphate-buffered saline pH 7.4 (PBS). The tissues were fixed with paraformaldehyde (4 %) in PBS for 20 min. The fixed sections were cryoprotected in increasing gradients of sucrose in PBS (5–20 %). Tissues were embedded in Tissue Tek (Miles Scientific, Naperville, IL, USA) and rapidly frozen in isopentane pre-cooled in liquid nitrogen. Cryosections were cut at 8 μm (Leica CM 3050), and endogenous peroxide was quenched by incubating the sections in 0.03 % hydrogen peroxide in PBS for 20 min. The sections were blocked in 1 % bovine serum albumin (BSA) containing 0.1 % Triton-X. Endogenous biotin was blocked with a biotin-blocking kit (Molecular Probes, Eugene, OR, USA) as per the manufacturer's instructions. Excess blocking serum was removed and sections were incubated with primary antibody (Kv4.2 or Kv4.3, diluted at 1:100) overnight at room temperature. The anti-Kv4.2 and anti-Kv4.3 antibodies were obtained commercially (Alomone Labs, Jerusalem, Israel) and have been utilized previously (e.g. Anderson *et al.* 2000; Zhang, T. T. *et al.* 2001). The Kv4.3 antibody recognizes the long and short forms of Kv4.3. Biotinylated goat anti-rabbit immunoglobulin and horseradish peroxidase-conjugated antibiotin antibody were applied to the sections for 30 min at room temperature. Peroxidase activity was visualized by applying 3,3′-diaminobenzidine containing 0.05 % hydrogen peroxide for 5 min at room temperature, and a Haematoxylin counterstain was applied. The sections were rinsed in tap water, dehydrated, cleared and mounted with coverslips. Negative control sections were tested with each antibody and were processed as above except that primary antibodies were substituted with (1) PBS or (2) pre-absorbed antibody (2 h at room temperature with antigens supplied by Alomone Labs). Photomicrographs were made with a Nikon eclipse E600 microscope incorporating Normarski optics.

Drugs and chemicals

Flecainide (acetate salt), 4-AP, tetraethylammonium (TEA; chloride salt), N^{ω}-nitro-L-arginine (L-NNA) and atropine (sulphate salt) were dissolved in deionized water. Nicardipine (HCl) was dissolved in ethanol and glibenclamide was dissolved in DMSO. The final concentration of DMSO was less than 0.1 %, and had no effect at this concentration. During electrophysiological experiments, desired concentrations were obtained by further dilution in the bathing solution. These agents were applied after completion of control recordings by exchanging the external solution in a continuous fashion. Unless stated otherwise, all drugs and chemicals used were from Sigma (St Louis, MO, USA).

RESULTS

A-type K^+ currents in isolated antral myocytes

Outward currents were recorded from antral myocytes with the conventional whole-cell patch-clamp technique. To minimize contamination from calcium-activated currents (e.g. large-conductance, calcium-activated K^+ currents), we used an external solution containing Mn^{2+} (2 mM) and included BAPTA (10 mM) in the pipette solution (e.g. Koh *et al.* 1999*a*, *b*). From a holding potential of −80 mV, 500 ms step depolarizations to potentials between −80 and +40 mV evoked outward currents with inactivating and sustained components (Fig. 1*A*). The ionic basis of these outward currents was established by measuring the K^+ sensitivity of the reversal potential of currents activated by 50 ms depolarizations to 0 mV using test steps to potentials ranging from −100 to 0 mV. When extracellular K^+ was raised from 5 to 35 mM, the reversal potential shifted from −83 ± 1 mV to −32 ± 1 mV (corrected for junction potential; data not shown; $n = 4$). These values are close to those predicted for a pure K^+ current (−87 and −36 mV) and we conclude that the underlying channels are selective for K^+ under these experimental conditions.

From a holding potential of −40 mV, step depolarization evoked sustained outward currents that were devoid of the inactivating component observed from more negative holding potentials (Fig. 1*A* and *B*). To isolate the rapidly inactivating portion of the outward current, the sustained currents activated from a holding potential of −40 mV were subtracted from the mixed currents obtained from −80 mV (Fig. 1*C*). Using this method, we constructed an average peak current–voltage relationship (Fig. 1*D*; $n = 6$). At 0 mV, the amplitude of the peak current density was 30 ± 4 pA pF^{-1} ($n = 6$). Difference currents were also used to measure the activation and inactivation kinetics of the rapidly inactivating outward current. Activation kinetics were assessed by measuring the time to half-maximal current (Fig. 1*E*). Activation kinetics showed strong voltage dependence as the time to half-maximal current decreased from 14.9 ± 1.2 ms at −30 mV to 4.4 ± 0.1 ms at 0 mV ($n = 6$). After reaching a peak, the K^+ currents decayed mono-exponentially (Fig. 1*C* and *E*). At negative test potentials, the rate of inactivation increased with greater depolarization as the time constant of inactivation declined from 96.1 ± 1.3 ms at −30 mV to 81.2 ± 2.4 ms at −10 mV ($n = 6$). However, depolarizations to more positive test potentials slowed inactivation as time constants increased from 83.4 ± 2.6 ms at 0 mV to 99.3 ± 2.2 ms at

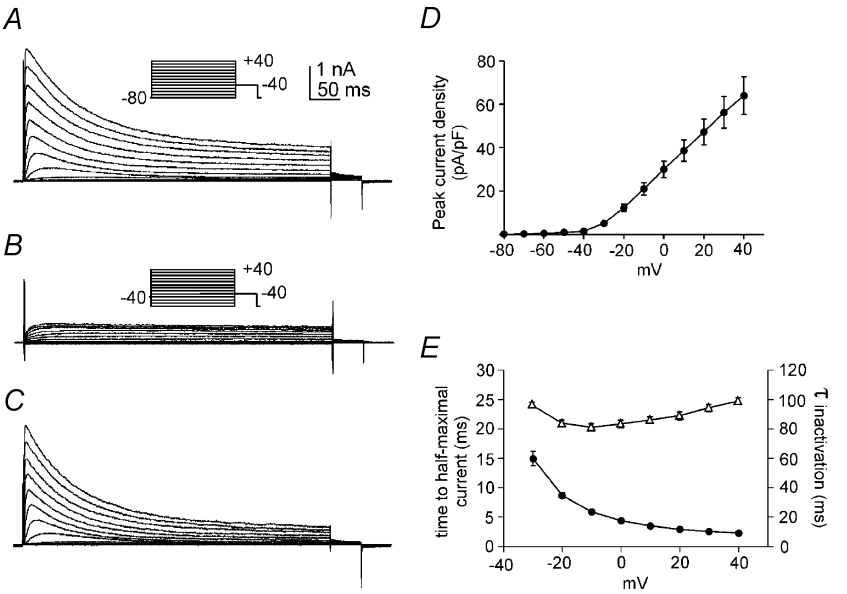

Figure 1. Isolation and characterization of A-type K^+ currents in antral myocytes

A and *B*, whole-cell A-type currents from holding potentials of −80 mV (*A*) and −40 mV (*B*). The membrane potential was stepped for 500 ms to potentials between −80 and +40 mV. *C*, difference currents obtained by subtracting currents in *B* from those in *A*. *D* and *E*, properties of difference currents (e.g. *C*) including peak current density as a function of voltage (*D*), time to half-maximum current (*E*, ●), and time constant of inactivation (*E*, △); $n = 6$ for each parameter. Error bars indicate S.E.M; where error bars are not visible, they are smaller than the symbols.

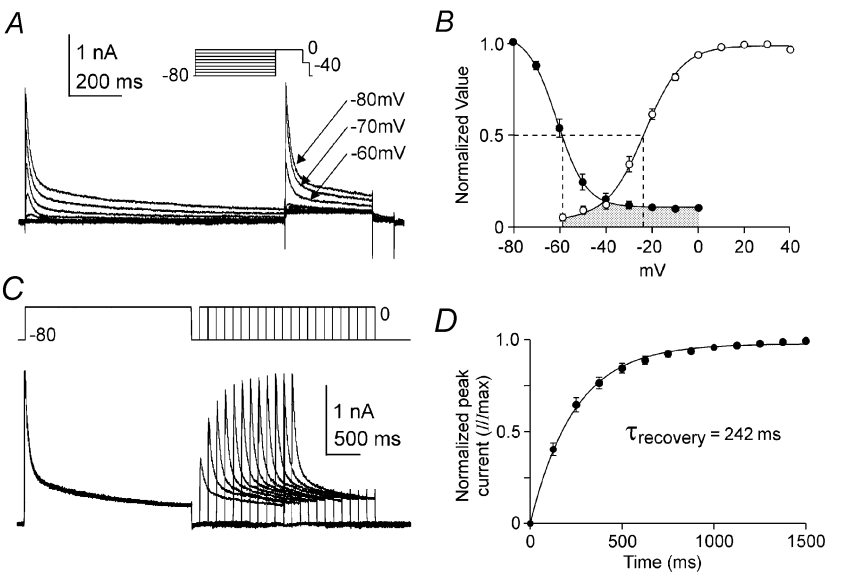

Figure 2. Antral A-type K^+ current availability and recovery from inactivation

A, membrane currents were measured at 0 mV following 3 s conditioning potentials ranging from −80 to 0 mV. *B*, steady-state inactivation is shown as a plot of normalized peak current (I/I_{max}) as a function of conditioning potential (●) and fitted with a Boltzmann function. For voltage dependence of activation, peak K^+ difference currents at test potentials between −80 and +40 mV (e.g. Fig. 1*D*) were converted into permeabilities using the Goldman-Hodgkin-Katz current equation. Permeabilities were normalized (P/P_{max}), plotted as a function of test potential (○) and fitted with a Boltzmann function. Dashed lines mark the voltages of half activation and inactivation ($n = 7$). *C*, the membrane potential was stepped for 2.5 s from −80 to 0 mV followed by a repolarization to −80 mV; recovery from inactivation was assessed by stepping the membrane potential back to 0 mV following variable recovery intervals at −80 mV. *D*, normalized peak currents (I/I_{max}) were plotted as a function of recovery interval and fitted with a single exponential function. $\tau_{recovery}$ is the time constant of recovery from inactivation ($n = 8$).

+40 mV. The fast activation and inactivation kinetics of this voltage-dependent K^+ current is consistent with classification as an A-type K^+ current.

A double-pulse protocol was used to determine the voltage dependence of inactivation of antral A-type currents (Fig. 2*A*). Currents evoked by depolarizations to a test potential of 0 mV decreased as the conditioning potential shifted from −80 to −50 mV. A plot of normalized peak current (I/I_{max}) as a function of conditioning potential (Fig. 2*B*) was fitted with a Boltzmann function. The voltage of half-inactivation of the A-type current was −65 ± 0.3 mV after correction for junction potential, and the slope of the Boltzmann function was −6.2 ± 0.2 mV ($n = 7$). To examine the voltage dependence of activation, peak difference currents were converted into permeabilities with the Goldman-Hodgkin-Katz current equation, normalized, and plotted as a function of test potential (Fig. 2*B*). Fitting this data with a Boltzmann function gave a voltage of half-activation of −26.5 ± 0.5 mV, after correction for junction potential, with a slope of 7.9 ± 0.5 mV ($n = 7$). There was significant activation and incomplete inactivation of the A-type current at potentials positive to −60 mV (Fig. 2*B*, shaded region), which is consistent with sustained current availability (i.e. window current) in this physiologically relevant potential range.

A double-pulse protocol was used to characterize the time required for recovery from inactivation of the A-type current at −80 mV (Fig. 2*C*). Following a 2.5 s conditioning pulses to 0 mV, the membrane potential was stepped back to −80 mV for recovery periods of variable duration. Recovery was determined by stepping the membrane potential back to 0 mV and plotting the normalized peak test current as a function of recovery interval (Fig. 2*D*). The time course of recovery from inactivation was well fitted with a single exponential of 252 ± 25 ms ($n = 8$). The voltage dependence of activation and inactivation and the rapid recovery from inactivation are also consistent with an A-type current. In addition, the speed of recovery from inactivation is characteristic of A-type currents formed by the Kv4 family of K^+ channels (e.g. Serodio *et al.* 1994).

Sensitivity of antral A-type currents to inhibition by 4-AP, flecainide and TEA

We examined A-type current sensitivity to inhibition by 4-AP, flecainide and TEA. 4-AP (10 mM) reduced peak A-type currents at test potentials of −20 mV and greater (Fig. 3*A* and *B*; $P < 0.05$; $n = 6$). Characteristic features of 4-AP-difference currents (Fig. 3*C*) include a rapid initial rise and peak followed by a decline to levels below baseline. Inhibition of peak A-type current by 4-AP is summarized in the current density–voltage relationship plotted in Fig. 3*D* ($n = 6$). Previous studies have demonstrated the inhibitory effect of flecainide on some A-type K^+ channels (Yeola & Snyders, 1997; see Rolf *et al.* 2000). We tested the sensitivity of antral A-type currents to flecainide inhibition. Flecainide (20 μM) decreased peak and sustained components of the A-type current ($P < 0.05$; $n = 5$; Fig. 4*A* and *B*). The effects of flecainide on peak components were dose dependent, with an IC_{50} of 35.5 ± 0.7 μM for step depolarizations to 0 mV (Fig. 4*C* and *D*; $n = 5$). The effects of flecainide on sustained components were dose dependent, with an IC_{50} of 36.3 ± 4.1 μM (Fig. 4*C* and *D*; $n = 5$). Flecainide inhibition of peak and sustained components were superimposed, resulting in

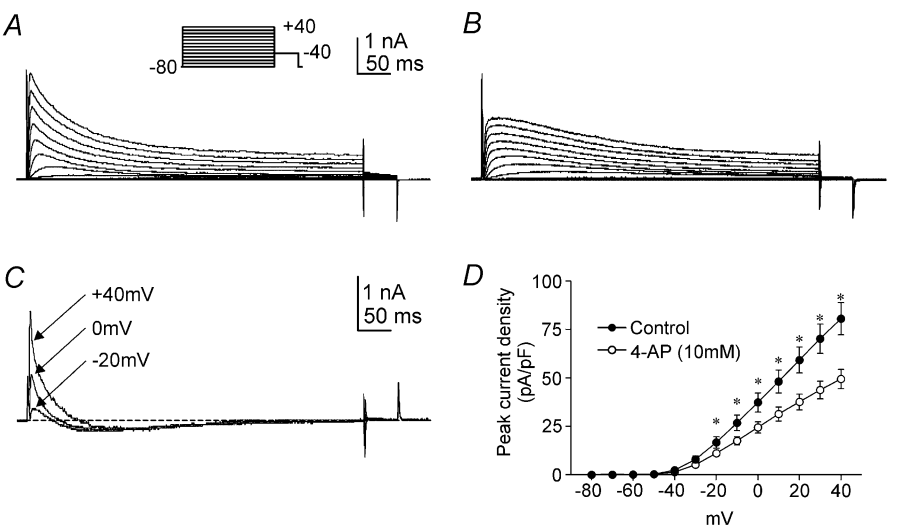

Figure 3. Effect of 4-aminopyridine (4-AP) on antral A-type currents

A and *B*, whole-cell A-type currents before (*A*) and after (*B*) external 4-AP (10 mM). The membrane potential was stepped for 500 ms from −80 mV to potentials between −80 and +40 mV. *C*, difference currents obtained by subtracting *B* from *A* at the voltage steps indicated; the dashed line marks zero current. *D*, average peak current density–voltage relationships before (○) and after 4-AP (●). *Significant reduction in peak current density after 4-AP as compared to control ($P < 0.05$; $n = 6$).

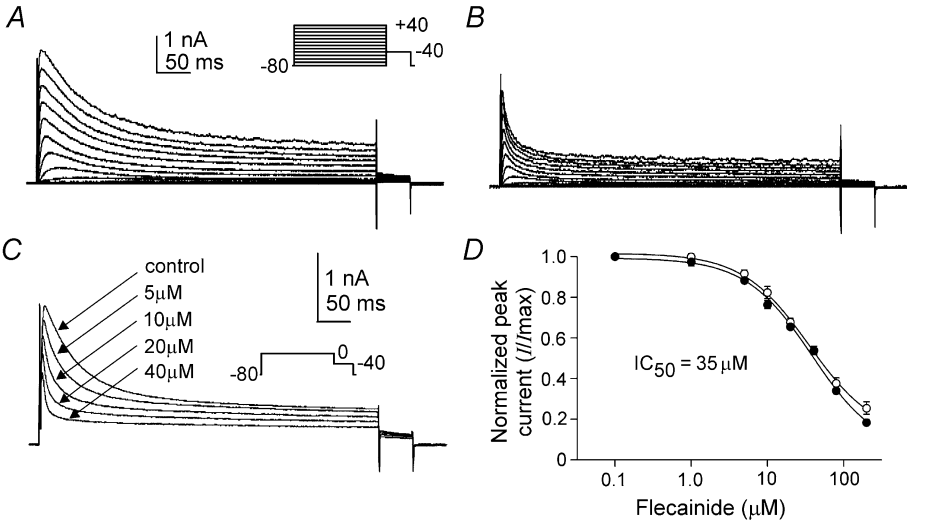

Figure 4. Inhibition of antral A-type currents by flecainide

A and *B*, whole-cell A-type currents before (*A*) and after (*B*) external flecainide (20 μM). The membrane potential was stepped for 500 ms from −80 mV to potentials between −80 and +40 mV. *C*, whole-cell A-type currents (steps to 0 mV from −80 mV) before and after increasing concentrations of flecainide as indicated. *D*, normalized peak (●) and sustained (○) currents at 0 mV (I/I_{max}; not shown) were plotted as a function of flecainide concentration (ranging from 0.1 to 200 μM), and fitted with a variable slope logistic equation, from which IC_{50} values of 35.5 ± 0.7 μM (peak) and 36.3 ± 4.1 μM (sustained) were determined (n = 5).

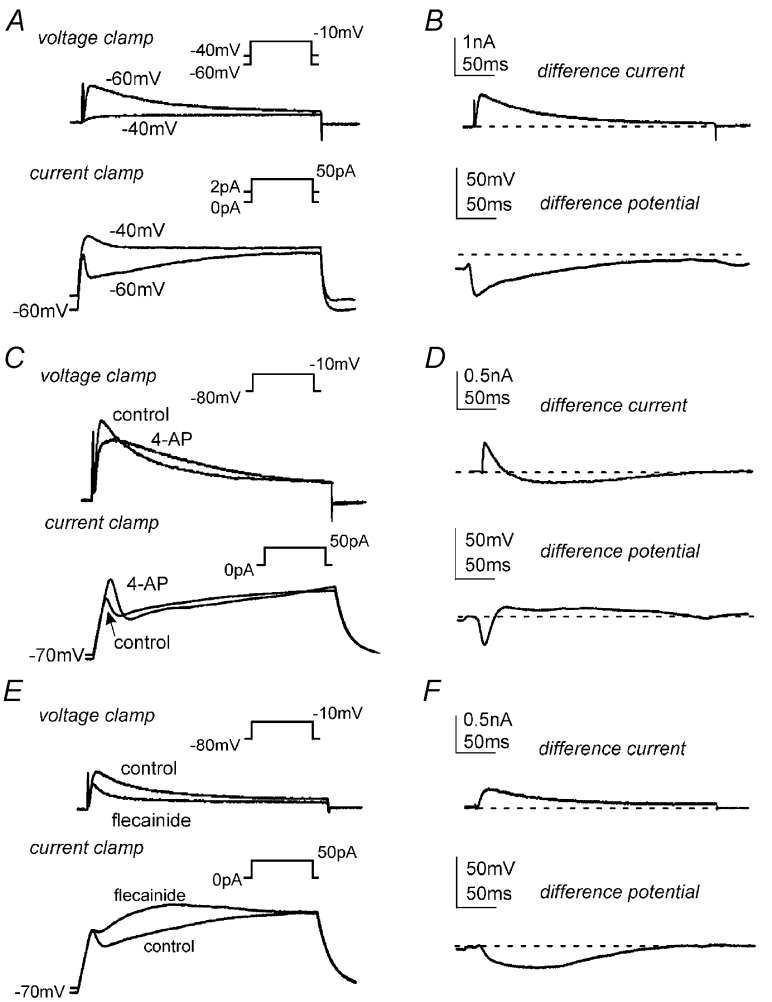

Figure 5. Effects of holding potential, 4-AP and flecainide on antral myocyte current-clamp recordings

A, in voltage-clamp mode, membrane currents were recorded at step depolarizations to −10 mV (500 ms) from holding potentials of −40 and −60 mV. In current-clamp mode, the membrane potential was held at −40 or −60 mV by continuous application of 1 or 2 pA of inward current, respectively. From these potentials, membrane voltage responses to 50 pA of depolarizing current (500 ms) were recorded. *B*, a difference current and difference potential was obtained by subtracting the appropriate −40 mV trace from the −60 mV trace; the dashed line marks zero current or zero potential. *C* and *E*, in voltage-clamp mode, membrane currents were recorded at step depolarizations to −10 mV (500 ms) from a holding potential of −80 mV before and after 4-AP (10 mM; *C*) or flecainide (30 μM; *E*). In current-clamp mode, membrane voltage responses to 50 pA of depolarizing current (500 ms) were recorded before and after 4-AP (10 mM; *C*) or flecainide (30 μM; *E*). *D* and *F*, a difference current and difference potential was obtained by subtracting the 4-AP (*D*) or flecainide (*F*) trace from the appropriate control trace; the dashed lines mark zero current or zero potential.

IC_{50} values that were not significantly different (Fig. 4*D*; $P > 0.05$; $n = 5$). In contrast to 4-AP and flecainide, TEA (10 mM) had no effect on antral A-type currents (data not shown; $P > 0.05$; $n = 6$).

Influence of A-type currents on the membrane potential of isolated antral smooth muscle cells

We investigated the contribution of A-type currents to membrane potentials of isolated antral myocytes in current-clamp mode. The voltage dependence of inactivation was used to characterize the effect of these currents on membrane responses to depolarization. From a holding potential of −60 mV (which is near the voltage of half-inactivation for the A-type current), step depolarizations evoked inactivating A-type currents; from −40 mV (where 80 % of the A-type current is inactivated) only non-inactivating currents were present (Fig. 5*A*, top). Myocytes were depolarized in current-clamp mode by injection of 50 pA current from holding potentials of −60 and −40 mV (Fig. 5*A*, bottom). The voltage response obtained from a holding potential of −60 mV was characterized by a rapid depolarization followed by a partial repolarization. When cells were initially held at −40 mV, the voltage response lacked the initial repolarization. Loss of transient repolarization from −40 mV corresponded temporally and in relative magnitude to the loss of the A-type current under voltage clamp from cells held at −40 mV. The differences in the voltage-clamp and current-clamp responses at holding potentials of −40 and −60 mV are shown as difference current and difference potentials in Fig. 5*B*.

Under current-clamp conditions, 4-AP (10 mM) depolarized the myocyte resting membrane potential from −68.8 ± 2.4 to −58.3 ± 3.5 mV ($P < 0.05$; $n = 4$). As demonstrated in the voltage-clamp recordings described above (and in Fig. 5*C*, top), following an initial reduction in outward current, 4-AP (10 mM) increased the outward current at points further along the depolarization pulse. In current-clamp mode (Fig. 5*C*, bottom), following injection of a 50 pA current, 4-AP resulted in an increase in initial depolarization (less outward current) as compared to control, with greater repolarization (more outward current) at points further into the depolarizing pulse. These observations are evident in the difference current and difference potential traces shown in Fig. 5*D*.

Similar to 4-AP, exposure to flecainide (30 μM) caused depolarization of the resting membrane potential from −71.4 ± 2.1 mV to −64.4 ± 1.4 mV ($P < 0.05$; $n = 5$). However, the effects of flecainide on A-type currents differed from those of 4-AP (above and Fig. 5). These differences carried over to current-clamp mode (Fig. 5*E*,

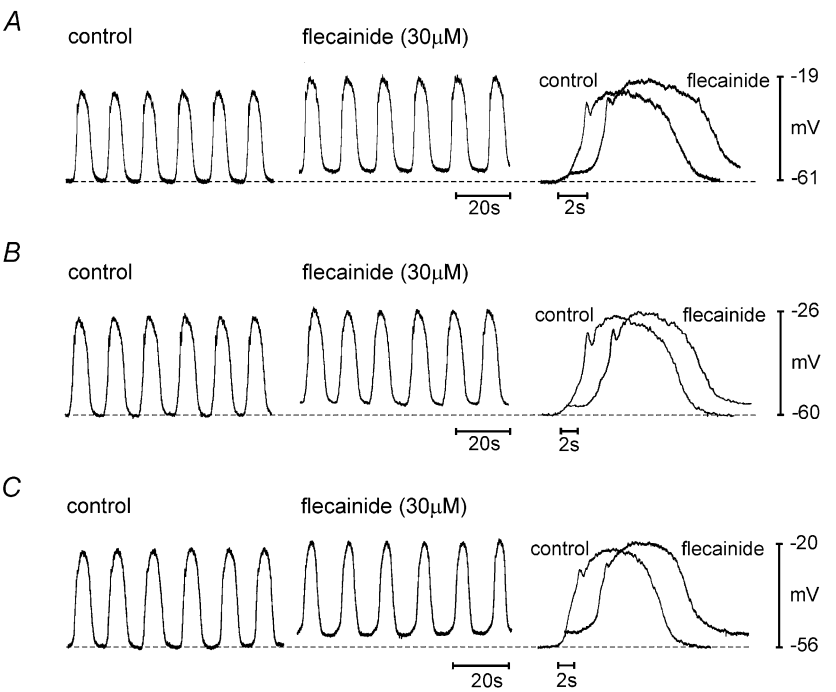

Figure 6. Effects of flecainide on the electrical activity of intact murine antral smooth muscle

A, flecainide (30 μM) was applied following control in standard oxygenated bathing solution (see Methods). *B* and *C*, in separate impalements, flecainide was applied as in *A*, but in the continued presence of bathing solution supplemented with N^{ω}-nitro-L-arginine (L-NNA), atropine and nicardipine (*B*) or supplemented with L-NNA, atropine, nicardipine, glibenclamide and TEA (*C*). For each panel, a representative slow wave before and after flecainide is shown at the right with an expanded time scale; for clarity, the flecainide slow wave has been shifted to the right by approximately 2 s. Dashed lines indicate the membrane potential between slow waves under control conditions.

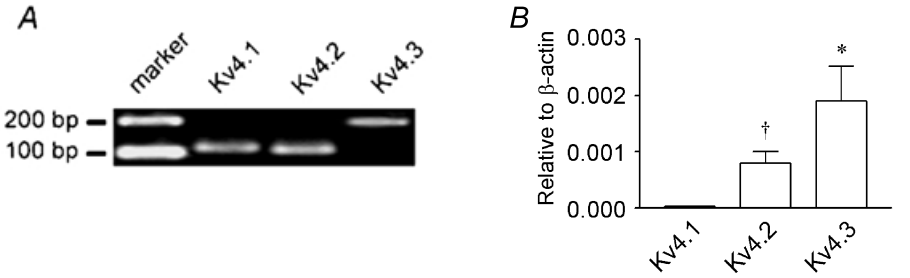

Figure 7. Quantification of Kv4 transcripts in antrum

A, detection of Kv4 transcripts in isolated antral myocytes. From left to right: 100 bp marker; Kv4.1 (amplicon = 116 bp); Kv4.2 (amplicon = 111 bp); Kv4.3, long isoform (amplicon = 176 bp). Amplicon identity was confirmed by DNA sequencing; see Methods for primer sequences. *B*, Kv4.1, Kv4.2 and Kv4.3 gene expression relative to β-actin in the antrum as determined by real-time PCR. *Significantly greater expression of Kv4.3 transcripts relative to Kv4.1 and Kv4.2 ($P < 0.05$; $n = 5$); †significantly greater expression of Kv4.2 transcripts relative to Kv4.1 ($P < 0.05$; $n = 5$).

bottom). In contrast to 4-AP, the initial depolarization following exposure to flecainide (30 μM) was identical to control, while depolarization was greater at points further into the depolarizing pulse (50 pA injection). These effects are reflected in the difference current and difference potential traces where the loss of outward current mirrors the loss in repolarization (Fig. 5*F*).

Influence of A-type currents on the electrical activity of intact antral smooth muscle

To determine the physiological relevance of our findings on isolated myocytes, we performed conventional microelectrode recordings on intact murine antral muscles. Spontaneous antral electrical activity (slow waves), described in detail elsewhere (e.g. Horiguchi *et al.* 2001; Kim *et al.* 2002), was recorded upon impalement of smooth muscle cells (Fig. 6). Inclusion of flecainide (30 μM) in the bathing solution depolarized the membrane potential between slow waves from −58.7 ± 1.3 to −53.1 ± 1.8 mV (Fig. 6*A*; $P < 0.05$; $n = 4$).

Since the effects of flecainide could be mediated through enteric neurons, we also tested the effects of flecainide in the presence of atropine (1 μM) and L-NNA (100 μM). Nicardipine (1 μM) was also included to block L-type Ca^{2+} channels. Under these conditions, flecainide depolarized the membrane potential between slow waves from −58.9 ± 3.7 to −54.1 ± 3.6 mV (Fig. 6*B*; $P < 0.05$; $n = 5$). In addition to A-type currents, flecainide has been shown to inhibit delayed rectifier (Follmer & Colatsky, 1990; Grissmer *et al.* 1994) and ATP-sensitive K^+ currents (K_{ATP}; Yunoki *et al.* 2001). To address this, in addition to atropine, L-NNA and nicardipine, we tested the effects of flecainide in the presence of TEA (10 mM) and glibenclamide (10 μM). With these agents in the bathing solution, flecainide (30 μM) depolarized the membrane potential between

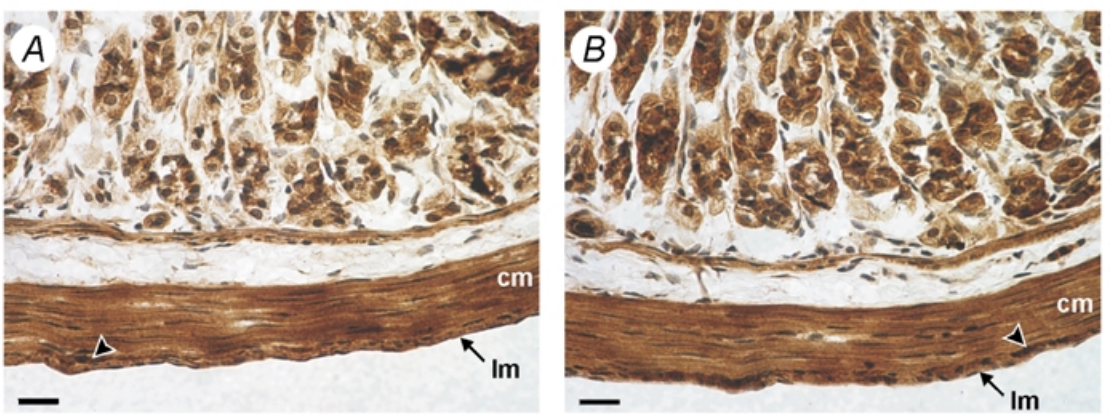

Figure 8. Kv4.2- and Kv4.3-like immunoreactivity in the tunica muscularis of the murine antrum

Haematoxylin counterstain. *A* and *B*, Kv4.2-like (*A*) and Kv4.3-like (*B*) immunoreactivity (in brown) throughout the circular (cm) and longitudinal (lm) muscle layers of the tunica muscularis in murine antrum. Arrowheads indicate Kv4-like immunoreactivity found within myenteric ganglia. Scale bars, 20 μm.

slow waves from −56.5 ± 2.9 to −51.7 ± 2.4 mV (Fig. 6*C*; $P < 0.05$; $n = 4$). Slow wave frequency, amplitude and duration, and features (amplitude and width) of the initial repolarizing 'notch' during the slow wave were not significantly altered by flecainide under any condition ($P > 0.05$).

Expression of Kv4 isoforms in antral smooth muscle

Previously, we demonstrated expression of Kv4 transcripts in murine colonic myocytes (Koh *et al.* 1999*b*). As in murine colon, the kinetic profile of A-type currents in the antrum resembles that of currents formed by the Kv4 family of K^+ channels (Serodio *et al.* 1994; Koh *et al.* 1999*b*; this study). Accordingly, we examined the expression of Kv4 channels in the antrum. Qualitative RT-PCR was used to detect Kv4 transcripts in isolated antral myocytes. Transcripts for each of the three Kv4 isoforms were found in isolated antral myocyte cDNA (Fig. 7*A*; $n = 4$). For each primer pair, only a single product of the correct size was visualized; amplicon identity was confirmed by DNA sequence analysis of gel-extracted products (data not shown). Although the primer pair for Kv4.3 flanked the alternatively spliced region of Kv4.3 (e.g. Ohya *et al.* 1997), we found only the long isoform of Kv4.3 in antral myocytes.

Relative expression levels of transcripts encoding each Kv4 isoform were determined by real-time PCR. To assess primer efficiency, standard curves (threshold cycle *vs.* $\log_{10}$ amplicon concentration, $\log_{10}$[amplicon]) were generated and slopes determined for each primer pair. The slopes obtained for the Kv4.1, Kv4.2 and Kv4.3 primer pairs were similar and were within the range of the calculated standard deviations for each pair ($P > 0.05$; $n = 3$). The efficiencies of each primer pair were thus considered equal, allowing for relative quantification of Kv4 transcripts. Relative quantifications were normalized between samples and PCR sessions using endogenous β-actin as a standard. As shown in Fig. 7*B*, murine antral smooth muscle possess transcripts encoding Kv4.3 in greater relative abundance than those encoding Kv4.1 and Kv4.2; Kv4.2 was more abundant than Kv4.1 ($P < 0.05$; $n = 5$ by one-way analysis of variance with Tukey's multiple comparison test).

We also used real-time PCR to assess antral expression of KChIPs (K^+ channel-interacting proteins), a group of known Kv4-specific auxiliary subunits (An *et al.* 2000). Where appropriate, the KChIP primer pairs were designed to amplify all known KChIP splice variants. The slopes obtained for the KChIP(1–4) primer pairs were similar and were within the range of the calculated standard deviations for each pair ($P > 0.05$; $n = 5$). Total KChIP transcript in antral smooth muscle was 0.0015 (relative to β-actin; $n = 5$), which is 2.5-fold lower than that reported for murine colon (Amberg *et al.* 2002; $P < 0.05$). In antrum, KChIP1 comprised 90 % of the total KChIP transcript ($P < 0.05$; $n = 5$).

Antibodies raised against specific epitopes of Kv4.2 and Kv4.3 channels were used to assess the expression of these channels in the murine antrum. An antibody for Kv4.1 was not available. In the antrum, strong Kv4.2- and Kv4.3-like immunoreactivities were observed in myocytes of the longitudinal and circular muscle layers of the tunica muscularis (Fig. 8). Obvious differences in expression levels of Kv4.2 and Kv4.3 were not apparent. Kv4-like immunoreactivity was also detected in non-smooth muscle cells. Two independent negative control experiments were performed to assess non-specific binding of Kv4 antibodies. First, immunoreactivity was not observed in control sections in which primary antibodies were omitted; second, immunoreactivity was absent in sections in which primary antibodies were pre-absorbed with purified control antigens (data not shown).

DISCUSSION

A-type K^+ currents have been observed in a variety of smooth muscles (Beech & Bolton, 1989; Imaizumi *et al.* 1989; Clapp & Gurney, 1991) including those of the GI tract (Smirnov *et al.* 1992; Vogalis *et al.* 1993; Akbarali *et al.* 1995; Koh *et al.* 1999*b*). Previously, we demonstrated the importance of A-type currents in maintaining the phasic nature of electrical activity in the murine colon (Koh *et al.* 1999*b*). In the present study, we identified and characterized an A-type current in myocytes isolated from the murine gastric antrum. In individual myocytes and in intact tissue preparations, this current contributes to maintenance of the resting membrane potential. We also provide pharmacological and molecular evidence indicating that Kv4 channels are the principal molecular entity underlying A-type currents in the antral smooth muscle cells.

In antral myocytes, inactivating A-type K^+ currents dominate macroscopic voltage-clamp recordings when calcium-activated K^+ currents are minimized. For voltage-gated currents, the degree of available current is a function of the intrinsic voltage-dependent properties of underlying channels and of the voltage range in which the tissue operates. In murine antrum, the maximum membrane potential between slow waves (i.e. resting potential) is approximately −60 mV (e.g. Horiguchi *et al.* 2001; Kim *et al.* 2002; this study). The voltage of half-inactivation for antral A-type current (−65 mV) is near this potential, indicating that a substantial fraction of this current is available at potentials achieved between slow waves. Small changes in membrane potential will have large effects on the availability of this current due to the steep voltage dependence of inactivation in this voltage range. Although not appreciable at the gain used in the figures presented, we were able to resolve statistically significant outward currents at −60 mV. Thus a small fraction of the channels responsible for the A-type current are activated at the

resting potential. There is also a window current for A-type current over a range of potentials spanning the resting potential due to fractional activation and incomplete inactivation of the conductance. Because of the high input resistance of antral smooth muscle cells (Noack *et al.* 1992; Edwards *et al.* 1999), we suggest that this small window current could have significant effects on membrane potential.

To test this hypothesis, we used the current-clamp mode of the whole-cell patch-clamp technique to examine the passive membrane properties of antral myocytes. The resting membrane potential of these cells was −70 mV, which is approximately 10 mV more negative than that of intact tissue preparations. It is likely that this discrepancy results from a loss of calcium-dependent inward current secondary to the presence of Mn^{2+} in the external solution and BAPTA in the pipette. Application of flecainide or 4-AP, two distinct inhibitors of the antral A-type current (see Results), caused a 7–10 mV depolarization of isolated myocytes.

To relate these findings to the tissue level, we applied flecainide to intact antral tissue preparations. Flecainide exposure decreased the membrane potential between slow waves by approximately 5 mV. To rule out possible neurogenic contributions, we applied flecainide in the presence of atropine and L-NNA (plus nicardipine). Under these conditions, flecainide depolarized the membrane potential by approximately 5 mV. Flecainide has also been shown to inhibit delayed rectifier (Follmer & Colatsky, 1990; Grissmer *et al.* 1994) and K_{ATP} (Yunoki *et al.* 2001) channels, each of which have been implicated in contributing to the resting membrane potential in smooth muscle (e.g. Archer *et al.* 1998; Koh *et al.* 1998). To rule out possible contamination of our results by non-specific block of these channels, we tested the effects of flecainide after the addition of TEA (which had no effect on antral A-type current) and glibenclamide. Atropine, L-NNA and nicardipine were included as before. In the presence of this cocktail, flecainide significantly depolarized the resting potential.

Inward rectifier K^+ currents have been shown to contribute to the resting membrane potential in GI smooth muscle (Flynn *et al.* 1999). However, inhibition of inwardly rectifying K^+ channels by flecainide is an unlikely explanation for the observed depolarization. In cardiac myocytes, 300 μM flecainide, 10-fold greater than the concentration used in this study, had no effect on inward rectifier currents (Slawsky & Castle, 1994). We conclude that the depolarization between slow waves observed after exposure to flecainide results from inhibition of a non-neural A-type current. Antral interstitial cells of Cajal may possess flecainide-sensitive A-type currents, thus given the present information, we cannot rule out contributory effects from this cell type. However, the flecainide-induced depolarization of antral myocytes suggests that at least some of the effects of this compound are mediated through direct effects on smooth muscle cells.

Slow wave frequency, amplitude and duration, and the initial repolarizing 'notch', a characteristic feature of antral slow waves (e.g. Dickens *et al.* 1999; Kim *et al.* 2002), were not affected by flecainide. At first glance, this seems to differ from the current-clamp data, where inhibition of the A-type current with flecainide, or inactivating it with a change in membrane holding potential, eliminated the transient notch in voltage responses to depolarizing current injection. The difference in these observations is explained by the differences in time course of the slow wave and voltage responses to current injection. At room temperature (22–25 °C), antral A-type currents were inactivated within 1 s after the onset of depolarization. A-type currents inactivate even more rapidly at physiological temperatures (e.g. 37 °C; Connor & Stevens, 1971; Huguenard *et al.* 1991). The relatively slow rate of depolarization from the resting potential to the peak of the upstroke of antral slow waves (> 1 s; see Fig. 6, at right) suggests that the A-type currents would be fully inactivated during the upstroke depolarization. Thus, current evoked via this conductance would not be available to participate in the partial repolarization (notch) in antral slow waves. It is therefore not surprising that inhibition of A-type current in antrum does not alter the waveforms of slow waves.

The properties of A-type currents in the antrum resemble those present in the murine colon (Koh *et al.* 1999*b*). As in the colon, the kinetic and pharmacological profiles of the A-type current presented in this study suggest that Kv4 channels underlie the A-type current in antrum. Antral A-type currents recover from inactivation with time constants similar to those reported for expressed Kv4 channels (e.g. Yeola & Snyders, 1997; Franqueza *et al.* 1999). However, recovery from inactivation of antral A-type current is approximately 4-fold slower than recovery from inactivation of colonic A-type currents. KChIPs speed recovery from inactivation of Kv4-mediated A-type currents (An *et al.* 2000). Therefore, the slow recovery from inactivation of antral A-type currents may result from the 2.5-fold lower level of KChIP expression in antrum as compared to colon (Amberg *et al.* 2002; see below). The relative sensitivity of A-type currents to inhibition by flecainide has been used to distinguish between Kv1 and Kv4 channels: A-type currents formed by Kv4 channels are more sensitive to inhibition by flecainide ($IC_{50} < 50$ μM) than those formed by Kv1 channels (Grissmer *et al.* 1994; Yamagishi *et al.* 1995; Rolf *et al.* 2000). Antral A-type currents were sensitive to low micromolar concentrations of flecainide, with IC_{50} values for the peak and sustained components of the current at 35 and 36 μM, respectively. These concentrations of flecainide are well below levels reported to inhibit Kv1 channels

(e.g. Kv1.4) and are comparable with levels reported to inhibit Kv4 channels (cf. Yeola & Snyders, 1997). Concentration–response curves for peak and sustained components of the A-type current were superimposed, suggesting that a single population of K^+ channels (i.e. Kv4) is responsible for both components.

We observed the expression of Kv4 transcripts in isolated smooth muscle cells with qualitative RT-PCR. Kv4.3 transcripts can be alternatively spliced in some tissues (e.g. Ohya *et al.* 2001), but we detected only the long form in the murine antrum. Real-time PCR indicated a predominance of the Kv4.3 transcript relative to Kv4.1 and Kv4.2; however, substantial levels of Kv4.2 transcript were also present. We investigated the expression of Kv4.2 and Kv4.3 channels with immunohistochemistry, and in agreement with the results from PCR, Kv4.2- and Kv4.3-like immunoreactivities were observed in antral myocytes. Real-time PCR showed lower levels of KChIP transcripts in antral muscle than in the murine colon (this study; Amberg *et al.* 2002). Lower expression of KChIP may explain the slower time course for recovery from inactivation of antral A-type currents relative to the time course for recovery from inactivation we have observed in colonic myocytes (Koh *et al.* 1999*b*). In contrast to murine colon and jejunum, functional expression of Kv4 channels in antral muscle cells does not appear to depend on co-expression of KChIPs. It is possible that the functional expression of Kv4 channels in the antrum is regulated by other auxiliary subunits such as non-KChIP members of the neuronal Ca^{2+} sensor family (e.g. Nakamura *et al.* 2001), minK-related peptide 1 (Zhang, M. *et al.* 2001), and/or Kvβ subunits (Yang *et al.* 2001).

To conclude, antral myocytes possess a robust A-type K^+ current that appears to contribute to the resting membrane potential in antral smooth muscle cells. Evidence supporting this conclusion was obtained in isolated myocytes and in intact tissue preparations. The A-type current does not influence the properties of spontaneous slow waves in the antrum because the A-type conductance inactivates during the relatively slow time course of the slow wave upstroke. Kv4.2 and Kv4.3 channels appear to be the channel responsible for the A-type current in antrum, as suggested by functional, pharmacological and molecular evidence. General availability of inhibitors with greater specificity, and development of conditional knockout animals will be useful for furthering our understanding of the physiological functions of A-type currents in GI smooth muscle.

REFERENCES

Akbarali, H. I., Hatakeyama, N., Wang, Q. & Goyal, R. K. (1995). Transient outward current in opossum esophageal circular muscle. *American Journal of Physiology* **268**, G979–987.

Amberg, G. C., Koh, S. D., Hatton, W. J., Murray, K. J., Monaghan, K., Horowitz, B. & Sanders, K. M. (2002). Contribution of Kv4 channels toward the A-type potassium current in murine colonic myocytes. *Journal of Physiology* **544**, 403–415.

Amberg, G. C., Koh, S. D., Perrino, B. A., Hatton, W. J. & Sanders, K. M. (2001). Regulation of A-type potassium channels in murine colonic myocytes by phosphatase activity. *American Journal of Physiology – Cell Physiology* **281**, C2020–2028.

An, W. F., Bowlby, M. R., Betty, M., Cao, J., Ling, H. P., Mendoza, G., Hinson, J. W., Mattsson, K. I., Strassle, B. W., Trimmer, J. S. & Rhodes, K. J. (2000). Modulation of A-type potassium channels by a family of calcium sensors. *Nature* **403**, 553–556.

Anderson, A. E., Adams, J. P., Qian, Y., Cook, R. G., Pfaffinger, P. J. & Sweatt, J. D. (2000). Kv4.2 phosphorylation by cyclic AMP-dependent protein kinase. *Journal of Biological Chemistry* **275**, 5337–5346.

Archer, S. L., Souil, E., Dinh-Xuan, A. T., Schremmer, B., Mercier, J. C., El Yaagoubi, A., Nguyen-Huu, L., Reeve, H. L. & Hampl, V. (1998). Molecular identification of the role of voltage-gated K^+ channels, Kv1.5 and Kv2.1, in hypoxic pulmonary vasoconstriction and control of resting membrane potential in rat pulmonary artery myocytes. *Journal of Clinical Investigation* **101**, 2319–2330.

Barry, P. H. (1994). JPCalc, a software package for calculating liquid junction potential corrections in patch-clamp, intracellular, epithelial and bilayer measurements and for correcting junction potential measurements. *Journal of Neuroscience Methods* **51**, 107–116.

Beech, D. J. & Bolton, T. B. (1989). A voltage-dependent outward current with fast kinetics in single smooth muscle cells isolated from rabbit portal vein. *Journal of Physiology* **412**, 397–414.

Clapp, L. H. & Gurney, A. M. (1991). Outward currents in rabbit pulmonary artery cells dissociated with a new technique. *Experimental Physiology* **76**, 677–693.

Connor, J. A. & Stevens, C. F. (1971). Voltage clamp studies of a transient outward membrane current in gastropod neural somata. *Journal of Physiology* **213**, 21–30.

Dickens, E. J., Hirst, G. D. & Tomita, T. (1999). Identification of rhythmically active cells in guinea-pig stomach. *Journal of Physiology* **514**, 515–531.

Edwards, F. R., Hirst, G. D. & Suzuki, H. (1999). Unitary nature of regenerative potentials recorded from circular smooth muscle of guinea-pig antrum. *Journal of Physiology* **519**, 235–250.

Epperson, A., Bonner, H. P., Ward, S. M., Hatton, W. J., Bradley, K. K., Bradley, M. E., Trimmer, J. S. & Horowitz, B. (1999). Molecular diversity of Kv α- and β-subunit expression in canine gastrointestinal smooth muscles. *American Journal of Physiology* **277**, G127–136.

Farrugia, G. (1999). Ionic conductances in gastrointestinal smooth muscles and interstitial cells of Cajal. *Annual Review of Physiology* **61**, 45–84.

Flynn, E. R., McManus, C. A., Bradley, K. K., Koh, S. D., Hegarty, T. M., Horowitz, B. & Sanders, K. M. (1999). Inward rectifier potassium conductance regulates membrane potential of canine colonic smooth muscle. *Journal of Physiology* **518**, 247–256.

Follmer, C. H. & Colatsky, T. J. (1990). Block of delayed rectifier potassium current, IK, by flecainide and E-4031 in cat ventricular myocytes. *Circulation* **82**, 289–293.

Franqueza, L., Valenzuela, C., Eck, J., Tamkun, M. M., Tamargo, J. & Snyders, D. J. (1999). Functional expression of an inactivating potassium channel (Kv4.3) in a mammalian cell line. *Cardiovascular Research* **41**, 212–219.

Grissmer, S., Nguyen, A. N., Aiyar, J., Hanson, D. C., Mather, R. J., Gutman, G. A., Karmilowicz, M. J., Auperin, D. D. & Chandy, K. G. (1994). Pharmacological characterization of five cloned voltage-gated K^+ channels, types Kv1.1, 1.2, 1.3, 1.5, and 3.1, stably expressed in mammalian cell lines. *Molecular Pharmacology* **45**, 1227–1234.

Hagiwara, S., Kusano, K. & Saito, N. (1961). Membrane changes of *Onchidium* nerve cell in potassium-rich media. *Journal of Physiology* **155**, 470–489.

Horiguchi, K., Semple, G. S., Sanders, K. M. & Ward, S. M. (2001). Distribution of pacemaker function through the tunica muscularis of the canine gastric antrum. *Journal of Physiology* **537**, 237–250.

Horowitz, B., Ward, S. M. & Sanders, K. M. (1999). Cellular and molecular basis for electrical rhythmicity in gastrointestinal muscles. *Annual Review of Physiology* **61**, 19–43.

Huguenard, J. R., Coulter, D. A. & Prince, D. A. (1991). A fast transient potassium current in thalamic relay neurons: kinetics of activation and inactivation. *Journal of Neurophysiology* **66**, 1304–1315.

Imaizumi, Y., Muraki, K. & Watanabe, M. (1989). Ionic currents in single smooth muscle cells from the ureter of the guinea-pig. *Journal of Physiology* **411**, 131–159.

Kim, T. W., Beckett, E. A., Hanna, R., Koh, S. D., Ordog, T., Ward, S. M. & Sanders, K. M. (2002). Regulation of pacemaker frequency in the murine gastric antrum. *Journal of Physiology* **538**, 145–157.

Koh, S. D., Bradley, K. K., Rae, M. G., Keef, K. D., Horowitz, B. & Sanders, K. M. (1998). Basal activation of ATP-sensitive potassium channels in murine colonic smooth muscle cell. *Biophysical Journal* **75**, 1793–1800.

Koh, S. D., Perrino, B. A., Hatton, W. J., Kenyon, J. L. & Sanders, K. M. (1999*a*). Novel regulation of the A-type K^+ current in murine proximal colon by calcium–calmodulin-dependent protein kinase II. *Journal of Physiology* **517**, 75–84.

Koh, S. D., Ward, S. M., Dick, G. M., Epperson, A., Bonner, H. P., Sanders, K. M., Horowitz, B. & Kenyon, J. L. (1999*b*). Contribution of delayed rectifier potassium currents to the electrical activity of murine colonic smooth muscle. *Journal of Physiology* **515**, 475–487.

Leblanc, N., Wan, X. & Leung, P. M. (1994). Physiological role of Ca^{2+}-activated and voltage-dependent K^+ currents in rabbit coronary myocytes. *American Journal of Physiology* **266**, C1523–1537.

Nakamura, T. Y., Pountney, D. J., Ozaita, A., Nandi, S., Ueda, S., Rudy, B. & Coetzee, W. A. (2001). A role for frequenin, a Ca^{2+}-binding protein, as a regulator of Kv4 K^+-currents. *Proceedings of the National Academy of Sciences of the USA* **98**, 12808–12813.

Nelson, M. T. & Quayle, J. M. (1995). Physiological roles and properties of potassium channels in arterial smooth muscle. *American Journal of Physiology* **268**, C799–822.

Noack, T., Deitmer, P. & Lammel, E. (1992). Characterization of membrane currents in single smooth muscle cells from the guinea-pig gastric antrum. *Journal of Physiology* **451**, 387–417.

Ohya, S., Tanaka, M., Oku, T., Asai, Y., Watanabe, M., Giles, W. R. & Imaizumi, Y. (1997). Molecular cloning and tissue distribution of an alternatively spliced variant of an A-type K^+ channel α-subunit, Kv4.3 in the rat. *FEBS Letters* **420**, 47–53.

Ohya, S., Tanaka, M., Oku, T., Furuyama, T., Mori, N., Giles, W. R., Watanabe, M. & Imaizumi, Y. (2001). Regional expression of the splice variants of Kv4.3 in rat brain and effects of C-terminus deletion on expressed K^+ currents. *Life Sciences* **68**, 1703–1716.

Rolf, S., Haverkamp, W., Borggrefe, M., Musshoff, U., Eckardt, L., Mergenthaler, J., Snyders, D. J., Pongs, O., Speckmann, E. J., Breithardt, G. & Madeja, M. (2000). Effects of antiarrhythmic drugs on cloned cardiac voltage-gated potassium channels expressed in *Xenopus* oocytes. *Naunyn-Schmiedeberg's Archives of Pharmacology* **362**, 22–31.

Sanders, K. M. (1992). Ionic mechanisms of electrical rhythmicity in gastrointestinal smooth muscles. *Annual Review of Physiology* **54**, 439–453.

Serodio, P., Kentros, C. & Rudy, B. (1994). Identification of molecular components of A-type channels activating at sub-threshold potentials. *Journal of Neurophysiology* **72**, 1516–1529.

Slawsky, M. T. & Castle, N. A. (1994). K^+ channel blocking actions of flecainide compared with those of propafenone and quinidine in adult rat ventricular myocytes. *Journal of Pharmacology and Experimental Therapeutics* **269**, 66–74.

Smirnov, S. V., Zholos, A. V. & Shuba, M. F. (1992). A potential-dependent fast outward current in single smooth muscle cells isolated from the newborn rat ileum. *Journal of Physiology* **454**, 573–589.

Thornbury, K. D., Ward, S. M. & Sanders, K. M. (1992). Participation of fast-activating, voltage-dependent K^+ currents in electrical slow waves of colonic circular muscle. *American Journal of Physiology* **263**, C226–236.

Tierney, A. J. & Harris-Warrick, R. M. (1992). Physiological role of the transient potassium current in the pyloric circuit of the lobster stomatogastric ganglion. *Journal of Neurophysiology* **67**, 599–609.

Vogalis, F., Lang, R. J., Bywater, R. A. & Taylor, G. S. (1993). Voltage-gated ionic currents in smooth muscle cells of guinea pig proximal colon. *American Journal of Physiology* **264**, C527–536.

Walker, R. L., Hume, J. R. & Horowitz, B. (2001). Differential expression and alternative splicing of TRP channel genes in smooth muscles. *American Journal of Physiology – Cell Physiology* **280**, C1184–1192.

Yamagishi, T., Ishii, K. & Taira, N. (1995). Antiarrhythmic and bradycardic drugs inhibit currents of cloned K^+ channels, Kv1.2 and Kv1.4. *European Journal of Pharmacology* **281**, 151–159.

Yang, E. K., Alvira, M. R., Levitan, E. S. & Takimoto, K. (2001). Kvβ subunits increase expression of Kv4.3 channels by interacting with their C termini. *Journal of Biological Chemistry* **276**, 4839–4844.

Yeola, S. W. & Snyders, D. J. (1997). Electrophysiological and pharmacological correspondence between Kv4.2 current and rat cardiac transient outward current. *Cardiovascular Research* **33**, 540–547.

Yunoki, T., Teramoto, N., Naito, S. & Ito, Y. (2001). The effects of flecainide on ATP-sensitive K^+ channels in pig urethral myocytes. *British Journal of Pharmacology* **133**, 730–738.

Zhang, M., Jiang, M. & Tseng, G. N. (2001). minK-related peptide 1 associates with Kv4.2 and modulates its gating function: potential role as β subunit of cardiac transient outward channel? *Circulation Research* **88**, 1012–1019.

Zhang, T. T., Takimoto, K., Stewart, A. F., Zhu, C. & Levitan, E. S. (2001). Independent regulation of cardiac Kv4.3 potassium channel expression by angiotensin II and phenylephrine. *Circulation Research* **88**, 476–482.

Acknowledgements
This project was supported by a program project grant, DK41315.